Elastic properties of a diblock copolymer monolayer and their relevance to bicontinuous microemulsion

M. W. Matsen
Polymer Science Centre, University of Reading, Whiteknights, Reading RG6 6AF, United Kingdom

(Received 13 October 1998; accepted 17 November 1998)

A new self-consistent field theory (SCFT) method is introduced for evaluating the exact mean-field elastic properties of a diblock copolymer monolayer separating two immiscible homopolymer phases. The method is illustrated on ternary blends of *A*- and *B*-type homopolymers of equal size blended with *AB* diblock copolymers of symmetric composition. We make comparisons with weak- and strong-segregation calculations, as well as with an earlier less accurate SCFT-based calculation. These previous approaches are found to produce sizable degrees of inaccuracy, emphasizing the need for our improved method. To conclude, we address the significance of our calculation in the efforts to develop bicontinuous polymeric microemulsions. Our primary conclusion is that the molecular weight of the diblock copolymer must be small. © *1999 American Institute of Physics.* [S0021-9606(99)50608-9]

I. INTRODUCTION

Plastics are, without question, one of the most successful types of material ever developed. They can be inexpensive, strong, rigid, flexible, elastic, shock resistant, light weight, adhesive, transparent, insulative, reasonably conductive, heat resistant, and easy to process. This diverse range of properties is largely a result of the numerous chemically distinct units capable of polymerizing. Even still, far greater control of material properties could be achieved by blending polymers as well as altering their chemistry. Varying the composition of a multicomponent polymer alloy is an extremely precise and simple method of tuning the properties. Unfortunately, these macromolecules generate very little entropy of mixing, and thus they are severely prone to phase separation.

Block copolymers represent a possible solution to this immiscibility problem. They can act as a compatiblizer by forming a monolayer between the two polymers and reducing the interfacial tension to virtually zero. Ideally, they would produce a microemulsion where the blend is stabilized by the thermal fluctuations of its internal interface. The microemulsion would exhibit either a micellar or a bicontinuous morphology. The former produces an unbalanced blend where the minority component forms swollen micelles immersed in a continuous matrix of the majority component. More useful is the bicontinuous microemulsion with balanced volume fractions in which each domain forms a continuous network that spans the entire blend. Monte Carlo simulations by Müller and Schick[1] have predicted a stability region for bicontinuous microemulsion, and more recently, experiments by Bates *et al.*[2] produced both types of microemulsion from polyethylene and polyethylenepropylene. The pertinent course of action now is to develop a better understanding of microemulsions in order to determine optimal blend conditions.[3,4] For instance, there would be a tremendous advantage in reducing the copolymer concentration from the $\sim$10% required in the experiments, since this is by far the most costly component of the blend. Advances of this nature will be crucial in our efforts to improve the commercial viability of these polymer alloys.

Although microemulsions are new to polymeric systems, they have long been studied in the amphiphilic community, where incidentally a couple percent of surfactant can be enough to form a water/oil microemulsion. The behavior of conventional microemulsions is generally discussed in terms of the elastic properties of the surfactant monolayer. Provided the monolayer is not highly curved, its energy is well represented by the Helfrich form[5]

$$F_{\rm int}=\int d\mathcal{A}[\sigma+\lambda H+2\kappa H^2+\overline{\kappa}G], \tag{1}$$

where $H=(c_1+c_2)/2$ and $G=c_1c_2$ are the mean and Gaussian curvatures, respectively, expressed in terms of the principle curvatures, c_1 and c_2. The coefficients, σ, κ, and $\overline{\kappa}$, are the interfacial tension, bending modulus, and saddle-splay modulus, respectively, and the remaining coefficient is related to the spontaneous mean curvature, $H_0=-\lambda/4\kappa$. In principle, σ, λ, κ, and $\overline{\kappa}$ can be calculated from microscopic models, and from their values one can determine if a microemulsion will be stable. First of all, a stable microemulsion requires $\sigma\approx 0$ in order to produce an extensive amount of internal interface.[6] Also the average of H in a bicontinuous microemulsion should be close to zero,[6,7] which implies $\lambda\approx 0$. Calculations by Morse[8] and by Golubović[9] further suggest that bicontinuous microemulsions only occur when $\overline{\kappa}+\frac{10}{9}\kappa>0$, and that $-\overline{\kappa}\sim k_BT$ is required in order to produce reasonable domain sizes. Recent Monte Carlo simulations[10,11] support these predictions, but nevertheless there are numerous competing opinions regarding the appropriate conditions for microemulsion.[12,13] Hopefully, the study of polymeric microemulsions will help resolve this issue.

Several theoretical calculations have already examined the elastic properties of a diblock copolymer monolayer. Wang and Safran[14,15] calculated elastic moduli for saturated

monolayers (i.e., $\sigma=0$) in the strong-segregation limit, while Matsen and Schick[16] have considered the general case in the weak-segregation regime. However, neither approach is capable of treating the intermediate degrees of segregation characteristic of most experiments. This regime demands the use of self-consistent field theory (SCFT)[17–19] with its well proven track record for quantitatively accurate results. In response to this need, Laradji and Desai[20] employed SCFT to calculate σ and κ by examining the capillary modes of a diblock copolymer monolayer. However, they could not access λ since capillary fluctuations do not change the average curvature, nor $\overline{\kappa}$ because the integral, $\int d\mathcal{A}\, G$, is a topological constant.[8,10,11] Furthermore, their approach required an assumption regarding how the interfacial profile is distorted by capillary waves.

In this paper, we again examine the elastic properties of a diblock copolymer monolayer using SCFT. However, our approach is more direct and considerably simpler than that of Laradji and Desai. It also allows access to all the interfacial parameters in Eq. (1) and makes no assumptions beyond those of SCFT. Furthermore, it is capable of examining an impressive range of segregations (up to $\chi N\sim 10^3$), which allows us to check the accuracy of all the previous methods. We find the weak-segregation theory (WST) of Matsen and Schick[16] to be highly inaccurate, presumably due to an approximation[21,22] where the curvature dependence of the interfacial profile is ignored. The SCFT calculations of Laradji and Desai[20] are also found to be inaccurate at weak segregations and low copolymer concentrations. This can be attributed to their assumption that capillary waves only distort the interfacial profile self-affinely. At strong segregations, the behavior predicted by the brush calculations of Wang and Safran[14,15] is qualitatively consistent with our SCFT results, but for realistic experimental conditions, the strong-segregation theory (SST) is highly inaccurate. However, a SST calculation of our own for bare homopolymer/homopolymer interfaces does agree well with SCFT. We conclude by discussing the appropriate conditions for forming bicontinuous microemulsion.

II. THEORY

In this section, we formulate the self-consistent field theory (SCFT)[17–19,23] for a ternary blend consisting of A- and B-rich homopolymer domains separated by monolayers of AB diblock copolymer. The location of the interface is specified by a delta-type function, $I(\mathbf{r})$, defined so that $\int d\mathbf{r}\, I(\mathbf{r})$ is proportional to the interfacial area contained within an arbitrary integration volume. Each diblock is composed of N segments of which a fraction f forms the A block, and each ν-type homopolymer is composed of $N\alpha_{h\nu}$ segments ($\nu=A$ or B). The A and B segments are assumed to be incompressible and are defined based on a common segment volume, ρ_0^{-1}. The segments are also assumed to be completely flexible with statistical lengths, a_A and a_B, respectively, i.e., the unperturbed rms end-to-end length of the diblock molecule is $aN^{1/2}$ where $a\equiv(fa_A^2+(1-f)a_B^2)^{1/2}$.

To perform SCFT calculations for the ternary blend, we begin with the free energy functional,

$$\frac{NF}{k_BT\rho_0}=-\mathcal{Q}_c-z_{hA}\mathcal{Q}_{hA}-z_{hB}\mathcal{Q}_{hB}+\int d\mathbf{r}[\chi N\Phi_A(\mathbf{r})\Phi_B(\mathbf{r})-W_A(\mathbf{r})\Phi_A(\mathbf{r})-W_B(\mathbf{r})\Phi_B(\mathbf{r})-\Xi(\mathbf{r})(1-\Phi_A(\mathbf{r})-\Phi_B(\mathbf{r}))-\Psi(\mathbf{r})I(\mathbf{r})(\Phi_A(\mathbf{r})-\Phi_B(\mathbf{r}))]. \tag{2}$$

It is obtained using the grand canonical formalism developed in Ref. 24, where the chemical potential, $\mu_{h\nu}\equiv k_BT\ln z_{h\nu}$, controls the concentration of ν-type homopolymer. The usual Flory–Huggins parameter, χ, controls the immiscibility of the A and B segments.

To evaluate the functional $F[\Phi_A,\Phi_B,W_A,W_B,\Xi,\Psi]$, it is necessary to first calculate, for each molecular species, the partition function of an isolated chain with its A and B segments subject to the fields, $W_A(\mathbf{r})$ and $W_B(\mathbf{r})$, respectively. For the diblock copolymer, the single-chain partition function is given by

$$\mathcal{Q}_c=\int d\mathbf{r}\, q_c(\mathbf{r},s)q_c^\dagger(\mathbf{r},s) \tag{3}$$

evaluated for any $0<s<1$, where s is a parameter running from its A end to its B end. Equation (3) requires $q_c(\mathbf{r},s)$, the partition function for the $(0,s)$ portion of the diblock molecule with its s segment fixed at $\mathbf{r}$. It is obtained by solving the modified diffusion equation,

$$\frac{\partial}{\partial s}q_c(\mathbf{r},s)=\begin{cases}[\frac{1}{6}Na_A^2\nabla^2-W_A(\mathbf{r})]q_c(\mathbf{r},s), & \text{if } 0<s<f\\ [\frac{1}{6}Na_B^2\nabla^2-W_B(\mathbf{r})]q_c(\mathbf{r},s), & \text{if } f<s<1,\end{cases} \tag{4}$$

with the initial condition $q_c(\mathbf{r},0)=1$.[17] Also required is the analogous function, $q_c^\dagger(\mathbf{r},s)$, for the $(s,1)$ portion of the chain, which is calculated by solving the same differential equation except with the right-hand side multiplied by -1 and the initial condition $q_c^\dagger(\mathbf{r},1)=1$. The single-chain partition function for a ν-type homopolymer is given by

$$\mathcal{Q}_{h\nu}=\int d\mathbf{r}\, q_{h\nu}(\mathbf{r},s)q_{h\nu}(\mathbf{r},\alpha_{h\nu}-s). \tag{5}$$

evaluated for any $0<s<\alpha_{h\nu}$, where

$$\frac{\partial}{\partial s}q_{h\nu}(\mathbf{r},s)=\left[\frac{1}{6}Na_\nu^2\nabla^2-W_\nu(\mathbf{r})\right]q_{h\nu}(\mathbf{r},s), \tag{6}$$

with $q_{h\nu}(\mathbf{r},0)=1$.

Within the SCFT approximation, the free energy of the melt is approximated by the lowest extremum in $F[\Phi_A,\Phi_B,W_A,W_B,\Xi,\Psi]$. The functions at the extremum, which we denote as ϕ_A, ϕ_B, w_A, w_B, ξ, and ψ, must therefore satisfy

$$\phi_A(\mathbf{r})=-\frac{\mathcal{D}\mathcal{Q}_c}{\mathcal{D}w_A(\mathbf{r})}-z_{hA}\frac{\mathcal{D}\mathcal{Q}_{hA}}{\mathcal{D}w_A(\mathbf{r})}, \tag{7}$$

$$\phi_B(\mathbf{r})=-\frac{\mathcal{D}\mathcal{Q}_c}{\mathcal{D}w_B(\mathbf{r})}-z_{hB}\frac{\mathcal{D}\mathcal{Q}_{hB}}{\mathcal{D}w_B(\mathbf{r})}, \tag{8}$$

$$w_A(\mathbf{r})=\chi N\phi_B(\mathbf{r})+\xi(\mathbf{r})-\psi(\mathbf{r})I(\mathbf{r}), \tag{9}$$

$$w_B(\mathbf{r}) = \chi N \phi_A(\mathbf{r}) + \xi(\mathbf{r}) + \psi(\mathbf{r}) I(\mathbf{r}), \tag{10}$$

$$\phi_A(\mathbf{r}) + \phi_B(\mathbf{r}) = 1, \tag{11}$$

$$I(\mathbf{r})(\phi_A(\mathbf{r}) - \phi_B(\mathbf{r})) = 0. \tag{12}$$

Equations (7) and (8) identify $\phi_\nu(\mathbf{r})$ as the ν-type segment concentration, which separates naturally into copolymer and homopolymer contributions, $\phi_{c\nu}(\mathbf{r})$ and $\phi_{h\nu}(\mathbf{r})$, respectively. From the definitions in Eqs. (3) and (5), it follows that

$$\phi_{cA}(\mathbf{r}) = \int_0^f ds\, q_c(\mathbf{r},s) q_c^\dagger(\mathbf{r},s), \tag{13}$$

$$\phi_{cB}(\mathbf{r}) = \int_f^1 ds\, q_c(\mathbf{r},s) q_c^\dagger(\mathbf{r},s), \tag{14}$$

$$\phi_{h\nu}(\mathbf{r}) = z_{h\nu} \int_0^{\alpha_{h\nu}} ds\, q_{h\nu}(\mathbf{r},s) q_{h\nu}(\mathbf{r},\alpha_{h\nu}-s). \tag{15}$$

This solves Eqs. (7) and (8); to solve the remaining four equations—Eqs. (9)–(12), we adjust $w_A(\mathbf{r})$, $w_B(\mathbf{r})$, $\xi(\mathbf{r})$, and $\psi(\mathbf{r})$. We will only consider cases where the interface is uniform, which allows us to replace the function, $\psi(\mathbf{r})$, by a constant, ψ. Once these equations are satisfied, the free energy is obtain by inserting the solution into Eq. (2).

Before we can consider a diblock monolayer, we must solve the SCFT for the two homopolymer-rich phases. For a uniform phase, things simplify immensely.[24] The free energy for a volume $\mathcal{V}$ can be expressed as

$$\begin{aligned}\frac{NF_{\text{bulk}}}{k_BT\rho_0\mathcal{V}} = {} & \frac{\phi_{hA}}{\alpha_{hA}}\left(\ln\frac{\phi_{hA}}{\alpha_{hA}} - 1\right) + \frac{\phi_{hB}}{\alpha_{hB}}\left(\ln\frac{\phi_{hB}}{\alpha_{hB}} - 1\right) \\ & + \phi_{\text{bulk}}(\ln\phi_{\text{bulk}} - 1) + \chi N(\phi_{hA} + f\phi_{\text{bulk}})(\phi_{hB} \\ & + (1-f)\phi_{\text{bulk}}) - \frac{\mu_{hA}\phi_{hA}}{\alpha_{hA}k_BT} - \frac{\mu_{hB}\phi_{hB}}{\alpha_{hB}k_BT},\end{aligned} \tag{16}$$

where the bulk copolymer concentration satisfies $\phi_{\text{bulk}} = 1 - \phi_{hA} - \phi_{hB}$, and the homopolymer concentrations, $\phi_{h\nu}$, are determined by

$$\begin{aligned}\frac{\mu_{hA}}{\alpha_{hA}k_BT} = {} & \frac{\phi_{hA}}{\alpha_{hA}}\ln\frac{\phi_{hA}}{\alpha_{hA}} - \ln\phi_{\text{bulk}} - \chi N(1-f) \\ & \times(\phi_{hA} - \phi_{hB} - (1-2f)\phi_{\text{bulk}}),\end{aligned} \tag{17}$$

$$\begin{aligned}\frac{\mu_{hB}}{\alpha_{hB}k_BT} = {} & \frac{\phi_{hB}}{\alpha_{hB}}\ln\frac{\phi_{hB}}{\alpha_{hB}} - \ln\phi_{\text{bulk}} \\ & + \chi N f(\phi_{hA} - \phi_{hB} - (1-2f)\phi_{\text{bulk}}).\end{aligned} \tag{18}$$

The chemical potentials, μ_{hA} and μ_{hB}, must be adjusted so that the free energies, F^A_{bulk} and F^B_{bulk}, of the A- and B-rich homopolymer phases are equal (i.e., the necessary condition for coexistence). The bulk copolymer concentrations, ϕ^A_{bulk} and ϕ^B_{bulk}, of the two phases are generally different, but for the symmetric conditions examined in our study, they will be equal.

Once we have the conditions for coexisting homopolymer-rich phases, we examine an interface between them of area $\mathcal{A}$. To evaluate the elastic coefficients in the Helfrich expression, Eq. (1), we consider cylindrical ($m=1$) and spherical ($m=2$) interfaces. This is done by using the corresponding coordinate systems, and making the substitutions,

$$I(\mathbf{r}) \to \Delta\,\delta(r - r_0), \tag{19}$$

$$\int d\mathbf{r} \to \mathcal{A}\int_{r_0-\Delta}^{r_0+\Delta} dr \left(\frac{r}{r_0}\right)^m, \tag{20}$$

$$\nabla^2 \to \frac{\partial^2}{\partial r^2} + \frac{m}{r}\frac{\partial}{\partial r}. \tag{21}$$

Our choice of $I(\mathbf{r})$ fixes the radius of either the cylinder or sphere to be r_0. The SCFT is then applied to a shell centered about the interface with a width, 2Δ, chosen large enough such that the melt reaches bulk conditions by $r = r_0 \pm \Delta$; generally, $\Delta/aN^{1/2} \approx 1.5$ is sufficient. For the cylindrical geometry, $H = 1/2r_0$ and $G = 0$, while for the spherical interface, $H = 1/r_0$ and $G = 1/r_0^2$. Inserting this into Eq. (1) for F_{int} and equating that to the difference in the free energy of the monolayer and the coexisting homopolymer phases, $F - F_{\text{bulk}}$, gives

$$\frac{N(F - F_{\text{bulk}})}{k_BT\rho_0\mathcal{A}aN^{1/2}} = \begin{cases} \Sigma + \frac{1}{2}\Lambda C + \frac{1}{2}KC^2 & \text{for } m=1 \\ \Sigma + \Lambda C + (2K + \overline{K})C^2 & \text{for } m=2, \end{cases} \tag{22}$$

where we have defined the dimensionless quantities,

$$C = \frac{aN^{1/2}}{r_0}, \tag{23}$$

$$\Sigma = \frac{\sigma a^2 N}{k_BT\overline{N}^{1/2}}, \tag{24}$$

$$\Lambda = \frac{\lambda a N^{1/2}}{k_BT\overline{N}^{1/2}}, \tag{25}$$

$$K = \frac{\kappa}{k_BT\overline{N}^{1/2}}, \tag{26}$$

$$\overline{K} = \frac{\overline{\kappa}}{k_BT\overline{N}^{1/2}}. \tag{27}$$

These quantities are expressed in terms of $\overline{N} \equiv \rho_0^2 a^6 N$, the invariant polymerization index of the diblock copolymer; typical values of $\overline{N}$ range from 10^3 to 10^4.[25] Evaluating the left-hand side of Eq. (22) requires the ratio of our sample volume (i.e., $r = r_0 - \Delta$ to $r_0 + \Delta$) to interfacial area, which is given by

$$\frac{\mathcal{V}}{\mathcal{A}} = \begin{cases} 2\Delta & \text{for } m=1 \\ 2\Delta(1 + (\Delta/r_0)^2/3) & \text{for } m=2. \end{cases} \tag{28}$$

One last quantity of interest is the volume of excess copolymer per unit area of interface. This is given by

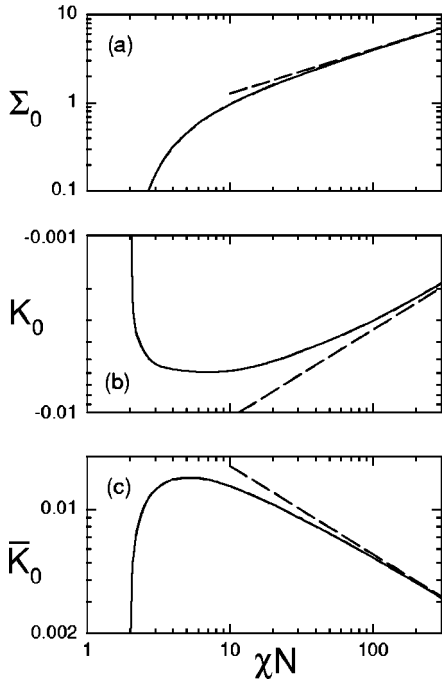

FIG. 1. Logarithmic plots of (a) surface tension, (b) bending modulus, and (c) saddle-splay modulus for a bare homopolymer interface vs χN, where here N is the polymerization index of the homopolymers (i.e., $\alpha=1$). SCFT results are shown with solid curves, and SST results are denoted with dashed lines.

$$\Omega=\frac{1}{aN^{1/2}}\int_{r_0-\Delta}^{r_0+\Delta}dr\left(\frac{r}{r_0}\right)^m(\phi_{cA}(r)+\phi_{cB}(r)-\Theta(r_0-r)\phi^A_{\rm bulk}-\Theta(r-r_0)\phi^B_{\rm bulk}), \quad (29)$$

where the step function, $\Theta(x)$, is 0 for $x<0$ and is 1 for $x>0$. (Note that we place the A-rich bulk phase on the inside of curvature.) Because Ω is curvature dependent, it is not a suitable measure of the copolymer content in the blend. For this purpose, we define Ω_0 as the excess copolymer of a flat interface.

In Appendix A, an efficient method is described for performing the above calculations using Fourier series expansions.

III. RESULTS

We have developed the SCFT to handle reasonably general blends in anticipation of future studies, but for now we will limit our attention to symmetric blends where $f=1/2$, $\alpha_{hA}=\alpha_{hB}\equiv\alpha$, and $a_A=a_B\equiv a$. Under these conditions, coexistence of the A- and B-rich homopolymer phases will occur at $\mu_{hA}=\mu_{hB}\equiv\mu$, both bulk copolymer concentrations will be equal (i.e., $\phi^A_{\rm bulk}=\phi^B_{\rm bulk}\equiv\phi_{\rm bulk}$), and there will be no spontaneous curvature (i.e., $\Lambda=0$).

Before considering ternary blends, we first examine the binary limit where the copolymer is removed (i.e., $\phi_{\rm bulk}=0$). Figure 1 plots the interfacial tension Σ_0, the bending modulus K_0, and the saddle-splay modulus $\bar{K}_0$ as a function of χN, where for now N is the degree of polymerization of each homopolymer (i.e., $\alpha=1$). All three quantities are zero at the critical point ($\chi N=2$). From there Σ_0 increases monotonically with χN, whereas the magnitudes of K_0 and $\bar{K}_0$ each display a rapid increase followed by a slow decay toward zero. A comparison to the SCFT results in Ref. 20 finds good agreement for Σ_0, but their values for K_0 have the opposite sign! We can only attribute this marked disagreement to the assumption in Ref. 20 that capillary waves cause self-affine deformations of the diblock monolayer.

The validity of our results can be supported with a comparison to strong-segregation predictions. In this limit, the interfacial energy is expressed as[26]

$$\frac{F_{\rm int,0}}{k_BT\rho_0\mathcal{A}}=\int dr\left(\frac{r}{r_0}\right)^m\left(\chi\phi_A(r)\phi_B(r)+\frac{a_A^2[\phi_A'(r)]^2}{24\phi_A(r)}+\frac{a_B^2[\phi_B'(r)]^2}{24\phi_B(r)}\right), \quad (30)$$

where the integral is minimized under the constraints, $\phi_B(r)=1-\phi_A(r)$ and $\phi_A(r_0)=1/2$. From the flat interface ($m=0$), we can obtain an analytical expression for Σ_0.[26] To determine K_0 and $\bar{K}_0$, we numerically integrate the Euler–Lagrange equations for cylindrical ($m=1$) and spherical ($m=2$) interfaces. In the symmetric case, $a_A=a_B\equiv a$, this gives

$$\Sigma_0=\left(\frac{\chi N}{6}\right)^{1/2}, \quad (31)$$

$$K_0=-\frac{0.0340}{(\chi N)^{1/2}}, \quad (32)$$

$$\bar{K}_0=\frac{0.0560}{(\chi N)^{1/2}}. \quad (33)$$

Note that the SST predictions for σ_0, κ_0, and $\bar{\kappa}_0$ are all independent of the homopolymer molecular weight. Most important, these SST results agree remarkably well with our SCFT calculations as demonstrated in Fig. 1.

Figure 2 examines how an interface saturated with diblock copolymer (i.e., $\Sigma=0$) is affected by interfacial curvature. The calculation is performed at $\alpha=1$ and $\chi N=50$, which corresponds to a strong degree of segregation and a reasonably dry monolayer as evident from the profiles shown in Figs. 2(c) and 2(d). Thus, we might expect the SST described in Appendix B to be valid, but our results illustrate that it is still inaccurate at this degree of segregation. The solid curves in Fig. 2(a) show the change in interfacial energy as the curvature is increased; the dashed curves denote the Helfrich approximation with $K=0.2884$ and $\bar{K}=-0.0926$. (Note that the SST predicts $K=0.596$ and $\bar{K}=-0.152$.) Remarkably, the Helfrich expression is accurate up to curvatures comparable to those of a micelle. This is, in part, because we are dealing with a symmetric blend where the interfacial energy is even in curvature, and thus the corrections to the Helfrich energy are only of order C^4. The solid curves in Fig. 2(b) show the change in excess copolymer caused by curving the interface, and the dashed curves are fits to $\Omega\approx\Omega_0+\Omega_2C^2$, with $\Omega_0=0.962$, $\Omega_2=-0.106$ for cylinders, and $\Omega_2=-0.360$ for spheres. (The respective values predicted in Appendix B by SST are 1.054, -0.183,

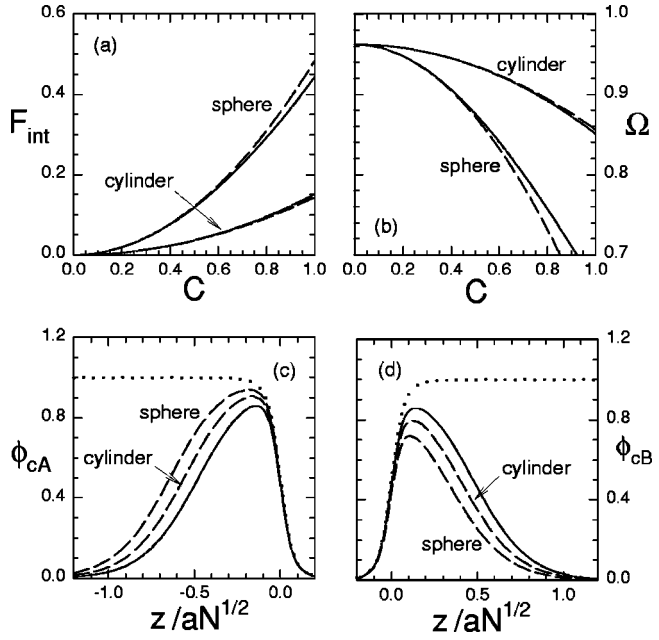

FIG. 2. Effects of curvature on a saturated diblock monolayer at $\alpha=1$ and $\chi N=50$. The solid curves in (a) and (b) show the change in interfacial energy [i.e., the left-hand side of Eq. (22)] and excess copolymer, respectively; the dashed curves correspond to quadratic fits. The brush profile of (c) the copolymer *A* blocks on the inside of curvature and (d) the copolymer *B* blocks on the outside of curvature. The solid curves show the profile for $C=0$ (flat interface) and the dashed curves are for $C=0.5$. The dotted curves in (c) and (d) show the overall *A*- and *B*-segment concentrations, respectively.

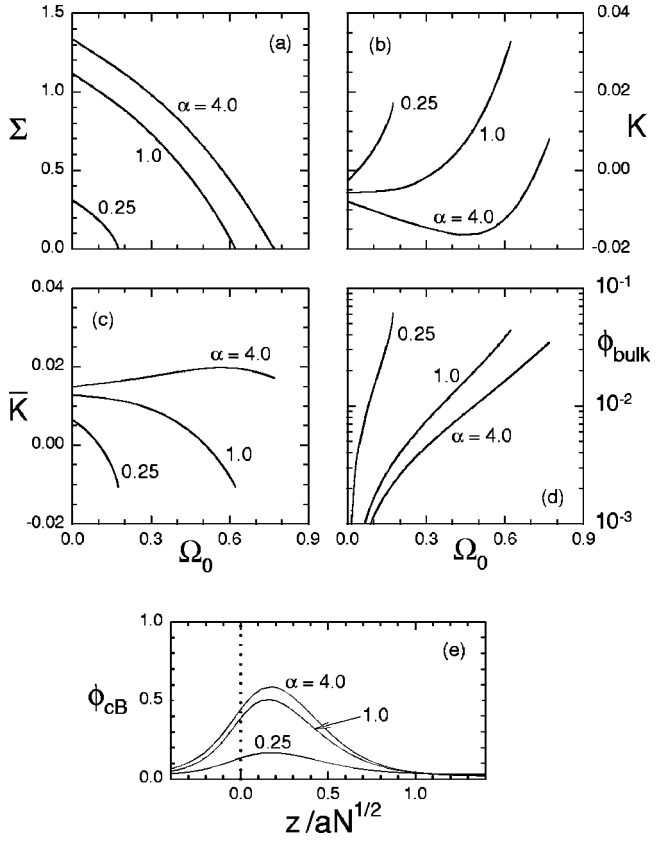

FIG. 3. (a) Interfacial tension, (b) bending modulus, and (c) saddle splay as a function of excess copolymer of a flat interface plotted for $\chi N=12$ and $\alpha=0.25$, 1.0, and 4.0. (d) Semilogarithmic plot of the bulk copolymer concentration as a function of excess copolymer. (e) Brush profiles of the flat, saturated monolayers (i.e., $C=0$ and $\Sigma=0$).

and -0.634.) Figures 2(c) and 2(d) demonstrate how curvature affects the brush profiles. The curvature causes the (*A*-block) interior brush to stretch, which forces some of the homopolymer out resulting in a dryer brush; the opposite occurs for the exterior (*B*-block) brush.

We now examine how the elastic properties change as the amount of copolymer is varied. Figure 3 displays results for $\chi N=12$ with $\alpha=0.25$, 1.0, and 4.0. In each case, the elastic coefficients are plotted from $\Omega_0=0$ (i.e., a bare interface) up to the point where the interface becomes saturated (i.e., $\Sigma=0$). The coefficients are expressed as a function of excess copolymer of the flat interface, Ω_0, rather than the bulk copolymer concentration, ϕ_{bulk}, because this makes comparisons more convenient and also because the SCFT underestimates ϕ_{bulk} by not accounting for the formation of micelles. Nevertheless, we plot ϕ_{bulk} vs Ω_0 in Fig. 3(d) so that one can convert between the two quantities. Also shown are the (*B*-block) brush profiles, $\phi_{cB}(r)$, for the flat saturated interfaces. Note, comparisons indicate that the accuracy of the results in Ref. 20, which is poor for the bare interface, improves as the interface becomes saturated with copolymer.

Figure 4 repeats the calculation in Fig. 3 except at a much higher degree of segregation, $\chi N=50$. The general behavior remains the same, but the magnitudes of the elastic coefficients change substantially. Although Σ has only increased by a factor of 2, K and $\bar{K}$ are approximately an order of magnitude larger. Also the bulk copolymer concentration is generally many orders of magnitude smaller, and the copolymer brushes are much dryer.

Figure 5 considers an even higher degree of segregation, $\chi N=200$, where we might expect strong-segregation theory (SST) to become accurate. Certainly this value of χN produces highly pure homopolymer phases and reasonably dry brushes as evident in Figs. 5(d) and 5(e), respectively. The dashed curves in Figs. 5(a)–5(c) denote the dry-brush SST predictions from Appendix B. These results are also plotted logarithmically in Fig. 6 to demonstrate the predicted scaling in Eqs. (B8)–(B10). The SST predictions should most closely match the large α limit of SCFT. Although there is qualitative agreement, significant inaccuracies in the SST still persist particularly for K and $\bar{K}$. Based on previous comparisons,[27] we suspect that χN must be several orders of magnitude larger before SST becomes quantitatively accurate.

IV. DISCUSSION

Our new method for calculating the elastic properties of a block copolymer monolayer represents a vast improvement over past techniques. It provides the exact mean-field values of σ, λ, κ, and $\bar{\kappa}$ using the well-established incompressible, Gaussian chain model.[18] This will be accurate for high molecular weights, but if need be, the calculation can be extended to treat semiflexible chains[19,28] and to include compressibility effects.[19,29] The mean-field approximation, which is normally very reliable for polymeric systems, will be par-

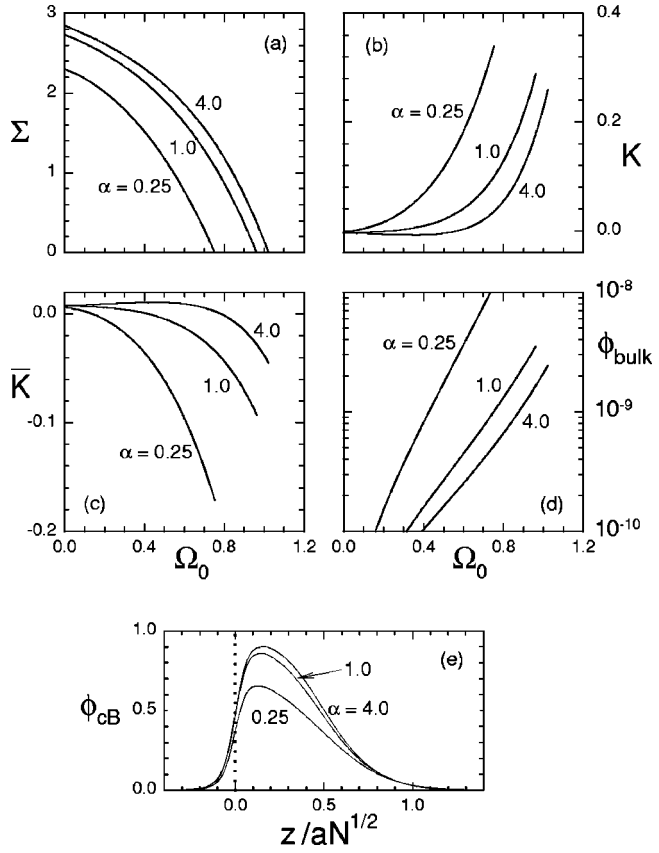

FIG. 4. Similar to Fig. 3, but calculated with $\chi N=50$.

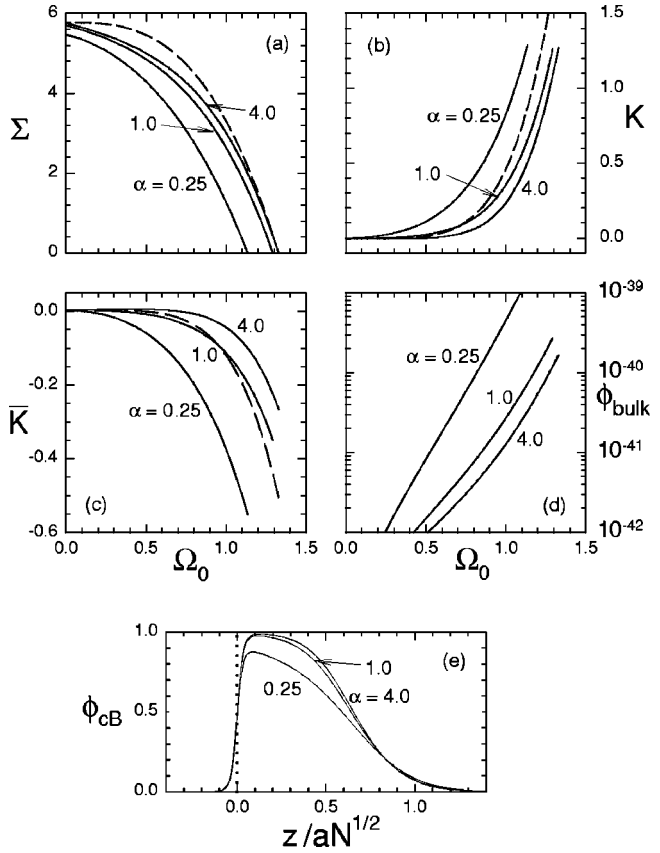

FIG. 5. Similar to Fig. 3, but calculated with $\chi N=200$. The SST predictions in Appendix B are shown with dashed curves in (a)–(c).

ticularly accurate in this case where we are examining constrained interfaces. There are also very few restrictions on the parameter space that can be accessed. Based on our previous experience,[27] our method should be capable of considering segregations in excess of $\chi N\sim 10^3$, which is well beyond values characteristic of experiment. Although, there are no restrictions on the relative molecular weights, inaccuracies will occur if one of the components starts to resemble a solvent.

We find that previous weak-segregation predictions by Matsen and Schick[16] for κ are highly inaccurate. For the conditions of their study, the actual values of κ are often negative, but the expression they used to evaluate κ excludes this possibility. The problem with this expression, which was developed in Refs. 21 and 22, is that it neglects the effect of curvature on the interfacial profile. Reference 21 acknowledges that this approximation affects κ and $\overline{\kappa}$, but they were unaware of how severe the resulting inaccuracy could be. In light of our present work, it is pointless to correct this approximation for polymeric systems since weak-segregation calculations are now obsolete. As we have already demonstrated, the SCFT approach of Laradji and Desai[20] produces similar degrees of inaccuracy, which again are a result of an invalid assumption of how curvature affects the interfacial profile. However, in this case, the approximation seems to improve as the interface becomes saturated with copolymer.

In the large χN limit, the copolymer junctions will become localized along a narrow interface and their blocks will become strongly stretched. The tendency of the blocks to contract will expel the homopolymer to produce a dry copolymer monolayer. In this situation, we can expect the dry-brush calculations in Appendix B to become relevant. However, we find that this is not an accurate picture even at $\chi N=200$; segregations such as $\chi N\sim 10^5$ are probably needed before the strong-stretching assumption becomes reliable.[27] Although the dry-brush theory remains quantitatively inaccurate even at very strong degrees of segregation, its predictions are still qualitatively correct. This is demonstrated in Table I, where we compare the SST predictions to our SCFT results for saturated monolayers ($\Sigma=0$) at $\chi N=200$. Except for small α, the SST is reasonably successful in predicting the ratio $(K-K_0)/(\bar{K}-K_0)$. Furthermore, the SST exponents, $\beta_\sigma=3$ and $\beta_\kappa=\beta_{\bar{\kappa}}=5$, for Ω_0 in Eqs. (B8)–(B10) agree favorably with our SCFT results, again provided α is not too small. Our SCFT values for β_α are obtained using

$$\beta_\sigma=\frac{\partial \ln(\sigma-\sigma_0)}{\partial \ln \Omega_0}, \tag{34}$$

evaluated for the saturated interfaces; analogous expressions are used for the other two exponents. For small homopolymers, where $\alpha\lesssim(\chi N)^{-1/3}$, the entropy of mixing homopolymer with the copolymer brush is significant relative to the stretching energy of the brush,[30] and consequently a wet-brush situation results. Therefore, we include wet-brush predictions[14,30] in Table I, but we note that such calculations are not really appropriate until the homopolymer concentra-

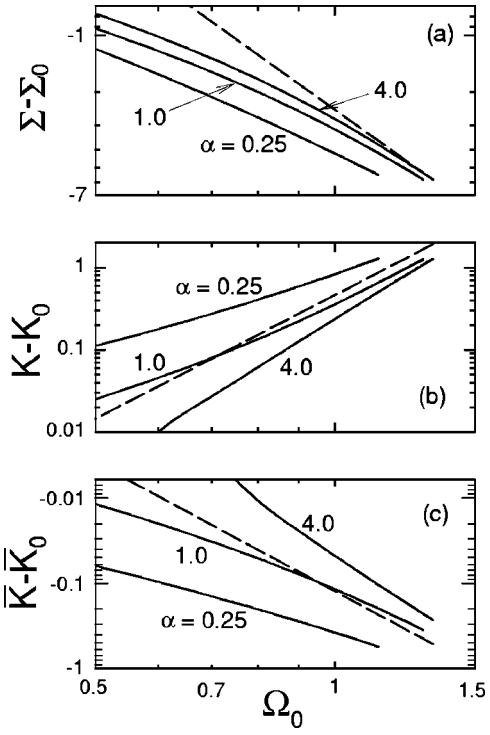

FIG. 6. Logarithmic plots of (a) interfacial tension, (b) bending modulus, and (c) saddle-splay modulus relative to those of the bare homopolymer interface vs the excess copolymer of a flat interface. The solid curves correspond to SCFT calculations for $\chi N=200$ with $\alpha=0.25$, 1.0, and 4.0, and the dashed curves represent the SST predictions in Appendix B.

tion dominates the brush.[31] Nevertheless, we can see a clear trend toward the wet-brush exponents as α decreases.

The elastic parameters will depend to some degree on the precise definition of the interface.[16,21,22] Shifting the position of the interface within the interfacial profile will cause small changes in the interfacial area and the principle curvatures. These must be compensated by changes in λ, κ, and $\bar{\kappa}$, since the interfacial energy $F_{\rm int}$ has to remain invariant. When the interface is broad, this can be an important issue given the significant leeway in defining the interface. Therefore, we have been careful to choose a sensible definition, i.e., the point where the *A*- and *B*-segment concentrations are equal. Note that the way we constrain the location of the interface in Eqs. (2) and (30) has to be consistent with our definition of the interface.

Perhaps the most valuable aspect of our calculation is its relevance to the stability of bicontinuous microemulsion. To address this issue, Table II lists the values of K and $\bar{K}$ for our saturated interfaces. An extra entry is also added for conditions corresponding to the experiment in Ref. 2. The column for $\bar{K}+\frac{10}{9}K$ is included because of its importance to microemulsion formation.[8,9] This quantity should be positive, which is true in each case. Given that, a lamellar phase should melt into a microemulsion, when the lamellar period swells above[8–10]

$$\xi_-=aN^{1/2}\exp(-\tfrac{6}{5}\pi\overline{KN}^{1/2}). \tag{35}$$

For the experiment of Bates *et al.*,[2] we estimate $-\bar{K}\approx 0.0025$ (see Table II) and $\bar{N}\approx 2.5\times 10^4$, which provides $\xi_-=4.4aN^{1/2}$. This is about 3.2 times the lamellar period of the neat diblock melt, and indeed this corresponds reasonably well with the degree of swelling required to melt the lamellar phase in their experiment.

A microemulsion will only be useful provided that its characteristic domain size, ξ_-, is reasonable, which requires $-\overline{KN}^{1/2}$ to be of order unity. A small ξ_- implies a large amount of interface and thus a large copolymer concentration, which is undesirable. On the other hand, ξ_- cannot be too large because the homopolymer phases should be mixed on a microscopic scale. The latter is of particular concern, since $-\overline{KN}^{1/2}$ tends to be large in polymeric systems. Based on our results, it is imperative that χN for the diblock copolymer should be small. Changing the homopolymer molecular weight (i.e., α) will have some effect on $-\overline{KN}^{1/2}$, but not much. Nevertheless, there are bound to be other effective ways of reducing $-\overline{KN}^{1/2}$. For instance, mixing in a small amount of shorter diblock copolymer should have a favorable effect,[32,33] much like the use of cosurfactants in classical water/oil microemulsions.[6] Chances are that other block copolymer architectures will provide superior elastic properties. In fact, Fredrickson and Bates[3] have already suggested ABC triblocks as a promising alternative to *AB* diblocks. We will address these possibilities in future publications.

There are other considerations besides the elastic properties of the monolayer. For instance, the block copolymer can only be effective if it prefers to remain at the interface as opposed to, e.g., forming small aggregates (i.e., micelles) in the homopolymer domains.[6] Previous calculations[34] suggest that these concerns are minimized when the diblock is symmetric ($f=1/2$). It is also crucial that there is no significant

TABLE I. Comparison between SST and SCFT for saturated monolayers ($\Sigma=0$) at $\chi N=200$.

α	$(\bar{K}-\bar{K}_0)/(K-K_0)$	β_σ	β_κ	$\beta_{\bar{\kappa}}$
0.0 (wet)[a]	−0.610	1.67	2.33	2.33
0.25	−0.430	2.00	3.56	3.10
1.0	−0.280	2.54	5.10	4.58
4.0	−0.211	2.77	5.77	5.98
∞ (dry)[a]	−0.267	3.00	5.00	5.00

[a]SST predictions for wet- and dry-brush conditions.

TABLE II. Elastic coefficients of saturated monolayers ($\Sigma=0$).

χN	α	K	$\bar{K}$	$\bar{K}+\frac{10}{9}K$
12[a]	0.2[a]	0.0038	−0.0025	0.0017
12	0.25	0.0170	−0.0107	0.0082
12	1.0	0.0328	−0.0105	0.0259
12	4.0	0.0079	0.0172	0.0260
50	0.25	0.340	−0.171	0.207
50	1.0	0.288	−0.093	0.227
50	4.0	0.259	−0.045	0.243
200	0.25	1.288	−0.551	0.880
200	1.0	1.260	−0.349	1.051
200	4.0	1.273	−0.265	1.149

[a]Conditions characteristic of the experiment in Ref. 2.

attraction between the monolayers. Such interactions would destroy the microemulsion by causing the monolayers to collapse into an ordered phase, probably lamellar given that we are considering situations where the spontaneous curvature is zero. This would expel the homopolymer, producing three-phase coexistence. Previous calculations[24,34–36] indicate that this becomes a problem at large α. These are the issues that we are presently examining.

V. SUMMARY

We have developed a method for evaluating the exact mean-field elastic coefficients of a diblock copolymer monolayer separating two immiscible homopolymer phases using the standard, incompressible, flexible-chain model.[18] The theory is developed for reasonably general conditions, but our initial study focuses on symmetric blends where the two homopolymer species are of equal size and the copolymer is of composition $f=1/2$. Our study spans the weak- to strong-segregation regimes (up to $\chi N=200$) and homopolymer to copolymer size ratios of $\alpha=0.25$ to 4.0. In this region of parameter space, we examine the homopolymer/homopolymer interface from zero copolymer concentration up to the saturation limit (i.e., zero surface tension).

Comparisons demonstrate that our method is a marked improvement over previous calculations. For example, we show that the weak-segregation calculations of Matsen and Schick[16] are highly inaccurate even at small χN. Furthermore, our method is simpler and more accurate than the previous SCFT approach of Laradji and Desai,[20] and it is able to access all the elastic coefficients of the interface. Our results also illustrate that the strong-segregation calculations of Wang and Safran[14,15] require extraordinary values of χN. Even at $\chi N=200$, the SST can only provide qualitative predictions.

According to the amphiphilic community, the formation of a microemulsion depends crucially on the elastic properties of its internal interface, although there is still some dispute over what those properties should be.[12,13] A leading opinion suggests that $K+\frac{10}{9}K$ must be positive and that $-KN^{1/2}$ should be of order unity.[8,10,12] We find that the first condition is generally satisfied, but that $-KN^{1/2}$ tends to be far too large. In the ternary blends considered in our study, the condition $-KN^{1/2}\sim 1$ requires the diblock copolymer molecular weight to be small. Further studies should examine whether altering the block copolymer architecture or blending block copolymers could improve the elastic properties.[3,4] We are presently examining other important issues such as the interaction between interfaces and the formation of micelles. Not only will such studies greatly aid in our efforts to improve polymeric microemulsions, they may also help to resolve some of the outstanding issues in the amphiphilic community regarding microemulsion behavior.

ACKNOWLEDGMENTS

We are grateful to D. C. Morse for discussions involving his excellent Review (Ref. 12) on sponge and microemulsion phases. The present work was supported by the Engineering and Physical Sciences Research Council (GR/M18034) and by the High Performance Computing Center at the University of Reading.

APPENDIX A: FOURIER REPRESENTATION OF SCFT

Here, we describe how to perform self-consistent field calculations in Fourier space, where all spatially dependent quantities, e.g., $g(r)$, are expanded in a Fourier series,

$$g(r)=\sum_{i=0}^{M} g_i f_i(r-r_0), \tag{A1}$$

where

$$f_i(z)=C_i\cos(i\pi(z+\Delta)/2\Delta). \tag{A2}$$

The normalization constants are chosen with $C_0=1$ and $C_i=\sqrt{2}$ for $i\neq 0$, so as to provide the convenient expression,

$$g_i=\frac{1}{2\Delta}\int_{-\Delta}^{\Delta} dz\, g(r_0+z) f_i(z), \tag{A3}$$

for the Fourier coefficients. In principle, the sum in Eq. (A1) should extend to infinity, but to perform a calculation we must truncate it at some large integer, M; values of $M\sim 500$ are feasible, but generally M can be far smaller without introducing any significant numerical inaccuracy.

To start the procedure, we must first calculate the Fourier coefficients of $R^{(m)}(r)\equiv(r/r_0)^m$ with $m=-1$, 1, and 2; this can be done explicitly when $m\neq -1$. For $i=0$, $R_0^{(1)}=1$ and $R_0^{(2)}=1+\frac{1}{3}(\Delta/r_0)^2$, and for $i\neq 0$,

$$R_i^{(1)}=\frac{2^{3/2}((-1)^i-1)}{i^2\pi^2}\left(\frac{\Delta}{r_0}\right), \tag{A4}$$

$$R_i^{(2)}=2R_i^{(1)}+\frac{2^{5/2}((-1)^i+1)}{i^2\pi^2}\left(\frac{\Delta}{r_0}\right)^2. \tag{A5}$$

We find that the best way to calculate the coefficients for $R^{(-1)}(r)$ is to solve the linear system of equations,

$$\sum_{i=0}^{M} R_i^{(-1)}\left[\sum_{j=0}^{M} R_j^{(1)}\Gamma_{ijk}\right]=\delta_{0k}, \tag{A6}$$

where

$$\Gamma_{ijk}=\frac{1}{2\Delta}\int_{-\Delta}^{\Delta} dz\, f_i(z)f_j(z)f_k(z) \tag{A7}$$

$$=\tfrac{1}{4}C_iC_jC_k[\delta_{i+j+k,0}+\delta_{i+j-k,0}+\delta_{i-j+k,0}+\delta_{i-j-k,0}]. \tag{A8}$$

Next the modified diffusion equations—Eqs. (4) and (6)—are written in matrix notation.[23] For a field $w_A(r)$, $\dot{q}_i(s)$ is related to $q_i(s)$ by the matrix

$$A_{ij}=-\frac{j^2\pi^2}{24}\left(\frac{aN^{1/2}}{\Delta}\right)^2\delta_{ij}-\frac{mj\pi}{12}\left(\frac{aN^{1/2}}{\Delta}\right)\times\left(\frac{aN^{1/2}}{r_0}\right)\sum_{k=0}^{M} R_k^{(-1)}\Gamma'_{ijk}-\sum_{k=0}^{M} w_{A,k}\Gamma_{ijk}, \tag{A9}$$

where $i,j=0,1,2,\ldots,M$ and

$$\Gamma'_{ijk}=\frac{1}{2\Delta}\int_{-\Delta}^{\Delta}dz\,f_i(z)\sqrt{2}\sin(j\pi(z+\Delta)/2\Delta)f_k(z) \tag{A10}$$

$$=\begin{cases}0 & \text{if } i+j+k \text{ is even}\\ C_i\sqrt{2}C_k[(i+j+k)^{-1}+(i+j-k)^{-1}-(i-j+k)^{-1}-(i-j-k)^{-1}]/2\pi & \text{otherwise.}\end{cases} \tag{A11}$$

The solution for $q_i(s)$ is then obtained with the transfer matrix,

$$T_A(s)\equiv\exp(As)=V_AD_AV_A^{-1}, \tag{A12}$$

where the columns of the matrix V_A contain the eigenvectors of A, and the elements of the diagonal matrix D_A are $\exp(\epsilon_i s)$, where ϵ_i are the eigenvalues of A. Of course, there is an analogous matrix, $T_B(s)$, corresponding to the field, $w_B(r)$. In terms of these matrices, the solutions to the diffusion equations are

$$q_{c,i}(s)=\begin{cases}T_{A,i0}(s) & \text{if } s<f\\ \sum_{j=0}^{M}T_{B,ij}(s-f)T_{A,j0}(f) & \text{if } f<s,\end{cases} \tag{A13}$$

$$q^{\dagger}_{c,i}(s)=\begin{cases}\sum_{j=0}^{M}T_{A,ij}(f-s)T_{B,j0}(1-f) & \text{if } s<f\\ T_{B,i0}(1-s) & \text{if } f<s,\end{cases} \tag{A14}$$

$$q_{h\nu,i}(s)=T_{\nu,i0}(s). \tag{A15}$$

Given these solutions, we evaluate the Fourier coefficients for the segment concentrations using

$$\phi_{cA,i}=\sum_{j,k=0}^{M}\Gamma_{ijk}\int_0^f ds\,q_{c,j}(s)q^{\dagger}_{c,k}(s), \tag{A16}$$

$$\phi_{cB,i}=\sum_{j,k=0}^{M}\Gamma_{ijk}\int_f^1 ds\,q_{c,j}(s)q^{\dagger}_{c,k}(s), \tag{A17}$$

$$\phi_{h\nu,i}=z_{h\nu}\sum_{j,k=0}^{M}\Gamma_{ijk}\int_0^{\alpha_{h\nu}}ds\,q_{h\nu,j}(s)q_{h\nu,k}(\alpha_{h\nu}-s). \tag{A18}$$

Next, $w_{A,i}$, $w_{B,i}$ and ψ are adjusted using a quasi-Newton–Raphson method so as to satisfy

$$w_{A,i}-w_{B,i}+\chi N(\phi_{A,i}-\phi_{B,i})+\psi C_i=0, \tag{A19}$$

$$\phi_{A,i}+\phi_{B,i}-\delta_{i,0}=0, \tag{A20}$$

$$\sum_{j=0}^{M}C_j(\phi_{A,j}-\phi_{B,j})=0, \tag{A21}$$

for $i=0,1,\ldots,M$. Once this is done, the free energy is given by

$$\frac{NF}{k_BT\rho_0\mathcal{A}aN^{1/2}}=\frac{2\Delta}{aN^{1/2}}\sum_{i=0}^{M}R_i^{(m)}\Big[q_{c,i}(1)+z_{hA}q_{hA,i}(\alpha_{hA})+z_{hB}q_{hB,i}(\alpha_{hB})+\sum_{j,k=0}^{M}(\chi N\phi_{A,j}\phi_{B,k}-w_{A,j}\phi_{A,k}-w_{B,j}\phi_{B,k})\Gamma_{ijk}\Big], \tag{A22}$$

and the excess copolymer is given by

$$\Omega=\frac{2\Delta}{aN^{1/2}}\sum_{i=0}^{M}R_i^{(m)}(\phi_{cA,i}+\phi_{cB,i})-\frac{r_0}{(m+1)aN^{1/2}}([1-(1-\Delta/r_0)^{m+1}]\phi^A_{\text{bulk}}+[(1+\Delta/r_0)^{m+1}-1]\phi^B_{\text{bulk}}), \tag{A23}$$

where $m=1$ for a cylindrical interface and $m=2$ for a spherical interface.

APPENDIX B: STRONG-SEGREGATION THEORY

Below, we derive the elastic coefficients for a diblock copolymer monolayer in the strong-segregation limit, where the highly stretched copolymers expel the homopolymer producing dry brushes. In this situation, the interfacial free energy is approximated as

$$F_{\text{int}}=F_{\text{int},0}+F^A_{\text{brush}}+F^B_{\text{brush}}-\mu_c\Omega\overline{N}^{1/2}\mathcal{A}/a^2N, \tag{B1}$$

where $F_{\text{int},0}$ is the energy of the bare A/B interface [i.e., Eq. (30)], F^A_{brush} is the stretching energy of the brush formed by the A blocks, F^B_{brush} is the same but for the B blocks, and μ_c is the chemical potential for introducing a copolymer molecule into the monolayer.

As before, we consider cylindrical ($m=1$) and spherical ($m=2$) interfaces of radius r_0. Assuming that A is on the inside of curvature, the stretching energy of the A blocks to second order in $C\equiv aN^{1/2}/r_0$ is[37]

$$\frac{F^A_{\text{brush}}}{k_BT\rho_0\mathcal{A}}=\frac{3\pi^2}{8f^2a_A^2N^2}\int_0^{h_A}dz\left(1-\frac{z}{r_0}\right)^m z^2 \tag{B2}$$

$$\approx\frac{\pi^2fa^3\Omega^3}{8a_A^2N^{1/2}}\left[1+\frac{3m}{4}f\Omega C+\frac{m(4+11m)}{20}(f\Omega C)^2\right], \tag{B3}$$

where the brush height, h_A, is related to the excess copolymer per unit area, Ω, by

$$h_A/aN^{1/2}=(1-(1-(m+1)f\Omega C)^{1/(m+1)})/C. \tag{B4}$$

The analogous expressions for the elastic energy of the B blocks is obtained by replacing a_A with a_B, f with $1-f$, and C with $-C$.

If we restrict ourselves to the symmetric case, $f=1/2$ and $a_A=a_B=a$, then the total interfacial energy is given by

$$\frac{N(F_{\rm int}-F_{\rm int,0})}{k_BT\rho_0\mathcal{A}aN^{1/2}}\approx\frac{\pi^2}{8}\Omega^3\left[1+\frac{m(4+11m)}{80}\Omega^2C^2\right]-\frac{\mu_c}{k_BT}\Omega. \tag{B5}$$

Because copolymer molecules in the monolayer are free to enter the bulk homopolymer phases, Ω will adjust to minimize $F_{\rm int}$. Thus, the excess copolymer will vary as

$$\Omega\approx\Omega_0\left[1-\frac{m(4+11m)}{96}\Omega_0^2C^2\right], \tag{B6}$$

where

$$\Omega_0=\left(\frac{8}{3\pi^2}\frac{\mu_c}{k_BT}\right)^{1/2} \tag{B7}$$

is the excess copolymer of a flat interface. Substituting Eq. (B6) into Eq. (B5), and comparing with Eq. (1) gives

$$\Sigma=\Sigma_0-\frac{\pi^2}{4}\Omega_0^3, \tag{B8}$$

$$K=K_0+\frac{3\pi^2}{64}\Omega_0^5, \tag{B9}$$

$$\overline{K}=\overline{K}_0-\frac{\pi^2}{80}\Omega_0^5. \tag{B10}$$

The above result is very similar to that of Wang and Safran,[14,15] except for four small issues. First, they ignore Σ_0, K_0, and $\overline{K}_0$. Second, their calculation is restricted to saturated interfaces where $\Sigma=0$. Third, they use a nonconventional definition of the elastic properties, where the interfacial energy is defined on a per copolymer basis rather than per unit area; consequently, their definitions of K and $\overline{K}$ vary as Ω_0^4 as opposed to Ω_0^5.[30,32] Fourth, they do not minimize their free energy under a constant copolymer chemical potential. They assume that there is no copolymer in the bulk phases to provide a constant chemical potential. Although this may be true at high degrees of segregation, the monolayer itself would still act as a copolymer reservoir, i.e., regions of different curvature should be in equilibrium and thus should have the same chemical potential. As a consequence, Wang and Safran get a slightly different expression for Ω, but in the symmetric case examined here, this does not affect the expressions for K and $\overline{K}$.

[1] M. Müller and M. Schick, J. Chem. Phys. **105**, 8885 (1996).
[2] F. S. Bates, W. W. Maurer, P. M. Lipic, M. A. Hillmyer, K. Almdal, and K. Mortensen, Phys. Rev. Lett. **79**, 849 (1997).
[3] G. H. Fredrickson and F. S. Bates, Eur. Phys. J. B **1**, 71 (1998).
[4] G. H. Fredrickson and F. S. Bates, J. Polym. Sci., Part B: Polym. Phys. **35**, 2775 (1997).
[5] W. Helfrich, Z. Naturforsch. C **28**, 693 (1973).
[6] P.-G. de Gennes and Taupin, J. Phys. Chem. **86**, 2294 (1982).
[7] R. Strey, Colloid Polym. Sci. **272**, 1019 (1994); Curr. Opin. Colloid Interface Sci. **1**, 403 (1996).
[8] D. C. Morse, Phys. Rev. E **50**, R2423 (1994).
[9] L. Golubović, Phys. Rev. E **50**, R2419 (1994).
[10] G. Gompper and D. M. Kroll, Phys. Rev. Lett. **81**, 2284 (1998).
[11] P. Pieruschka and S. Marčelja, Langmuir **10**, 345 (1994).
[12] D. C. Morse, Curr. Opin. Colloid Interface Sci. **2**, 365 (1997).
[13] G. Porte, Curr. Opin. Colloid Interface Sci. **1**, 345 (1996).
[14] Z.-G. Wang and S. A. Safran, J. Chem. Phys. **94**, 679 (1991).
[15] Z.-G. Wang and S. A. Safran, J. Phys. (France) **51**, 185 (1990).
[16] M. W. Matsen and M. Schick, Macromolecules **26**, 3878 (1993); **27**, 2316 (1994).
[17] E. Helfand, J. Chem. Phys. **62**, 999 (1975).
[18] M. W. Matsen and F. S. Bates, Macromolecules **29**, 1091 (1996).
[19] F. Schmid, J. Phys.: Condens. Matter **10**, 8105 (1998).
[20] M. Laradji and R. C. Desai, J. Chem. Phys. **108**, 4662 (1998).
[21] G. Gompper and S. Zschocke, Phys. Rev. A **46**, 4836 (1992).
[22] G. Gompper and S. Zschocke, Europhys. Lett. **16**, 731 (1991).
[23] M. W. Matsen and M. Schick, Phys. Rev. Lett. **72**, 2660 (1994).
[24] M. W. Matsen, Phys. Rev. Lett. **74**, 4225 (1995); Macromolecules **28**, 5765 (1995).
[25] F. S. Bates, M. F. Schulz, A. K. Khandpur, S. Förster, J. H. Rosedale, K. Almdal, and K. Mortensen, Faraday Discuss. **98**, 7 (1994).
[26] A. N. Semenov, Macromolecules **26**, 6617 (1993).
[27] M. W. Matsen and F. S. Bates, Macromolecules **28**, 8884 (1995).
[28] D. C. Morse and G. H. Fredrickson, Phys. Rev. Lett. **73**, 3235 (1994). M. W. Matsen, J. Chem. Phys. **104**, 7758 (1996).
[29] E. Helfand and Y. Tagami, J. Chem. Phys. **56**, 3592 (1972).
[30] L. Leibler, Makromol. Chem., Macromol. Symp. **16**, 1 (1988).
[31] S. T. Milner, T. A. Witten, and M. E. Cates, Macromolecules **21**, 2610 (1988).
[32] S. T. Milner and T. A. Witten, J. Phys. (France) **49**, 1951 (1988).
[33] N. Dan and S. A. Safran, Macromolecules **27**, 5766 (1994).
[34] R. Israels, D. Jasnow, A. C. Balazs, L. Guo, G. Krausch, J. Sokolov, and M. Rafailovich, J. Chem. Phys. **102**, 8149 (1995).
[35] K. R. Shull and E. J. Kramer, Macromolecules **23**, 4769 (1990).
[36] P. K. Janert and M. Schick, Macromolecules **30**, 137 (1997).
[37] A. E. Likhtmann and A. N. Semenov, Macromolecules **27**, 3103 (1994).